SUPPORTING INFORMATION

Photodynamic treatment of melanoma cells using aza-dipyrromethenes as photosensitizers

Kelly A. D. F. Castro,[a†*] Letícia D. Costa,[b†] Samuel Guieu,[b,c] Juliana C. Biazzotto,[a] Maria da Graça P. M. S. Neves,[b] M. Amparo F. Faustino,[b*] Roberto S. da Silva,[a*] and Augusto C. Tomé[b*]

[a] Department of Physics and Chemistry, Faculty of Pharmaceutical Sciences of Ribeirão Preto, University of São Paulo, SP, Brazil
[b] LAQV-REQUIMTE, Department of Chemistry University of Aveiro, Portugal
[c] CICECO – Aveiro Institute of Materials, Department of Chemistry, University of Aveiro, Portugal

Table of Contents

Synthesis

The ADPM **1-4** were synthesized following the procedures previously described in the literature.[1]
Nuclear magnetic resonance (NMR) spectra were recorded at room temperature on a Bruker Avance 300 spectrometer using $CDCl_3$ as solvent. Chemical shifts δ are reported in parts per million (ppm) relative to residual solvent protons (7.26 ppm) and the coupling constants (*J*) are given in Hertz (Hz).
Matrix-assisted laser desorption ionization (MALDI) time-of-flight/time-of-flight mass spectra were acquired on a Brucker Ultraflex TOF/TOF spectrometer operating in the positive mode.

Structural Characterization

Mass Spectrometry

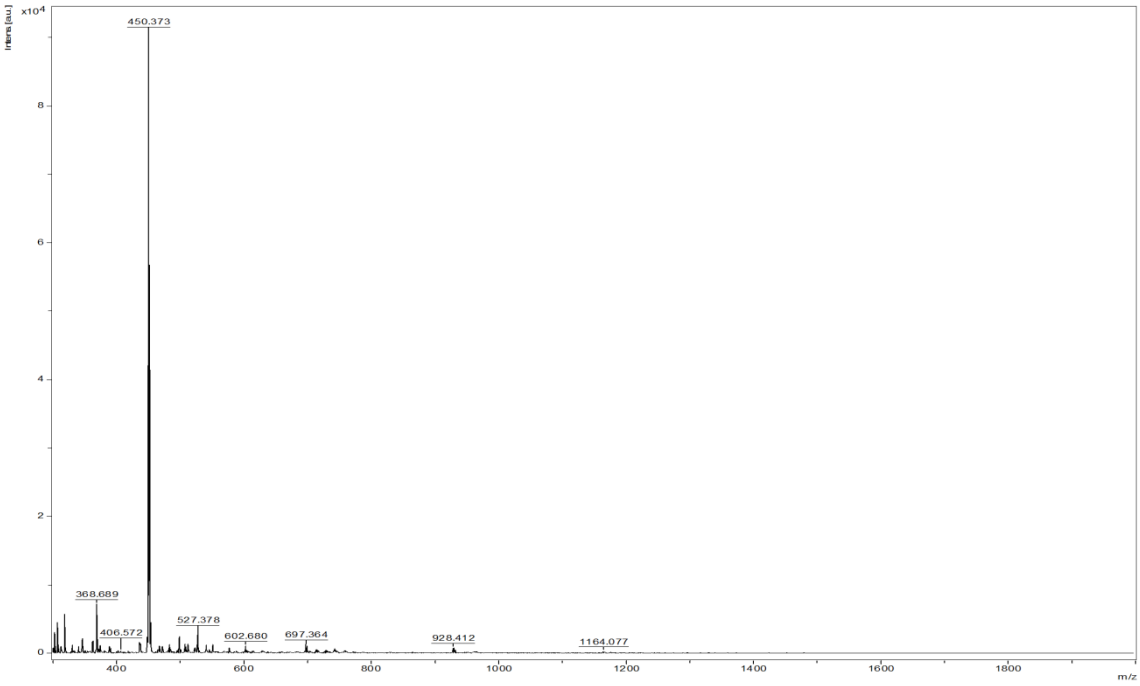

Figure S1. MALDI-TOF mass spectrum of ADPM **1**.

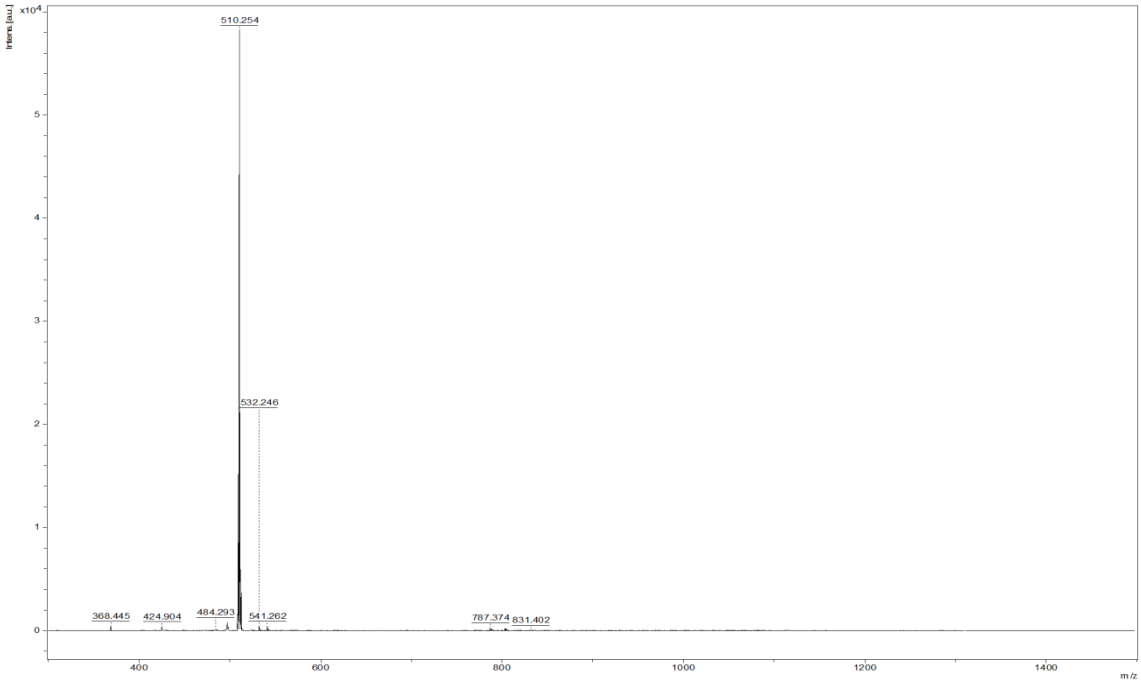

Figure S2. MALDI-TOF mass spectrum of ADPM **2**.

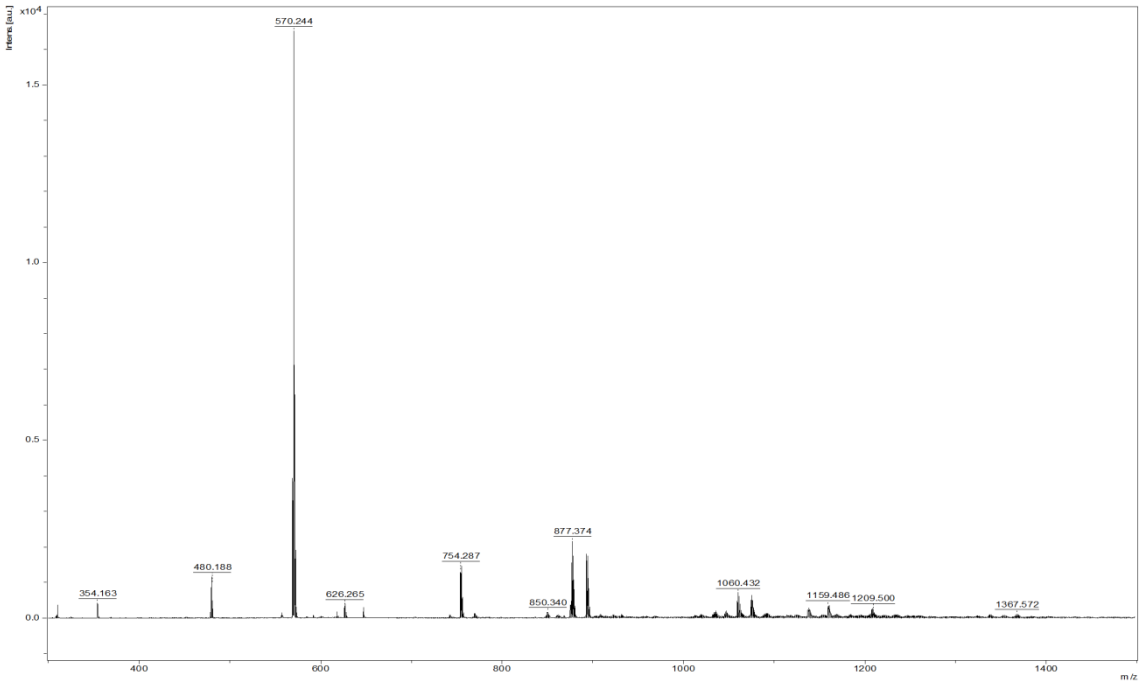

Figure S3. MALDI-TOF mass spectrum of ADPM **3**.

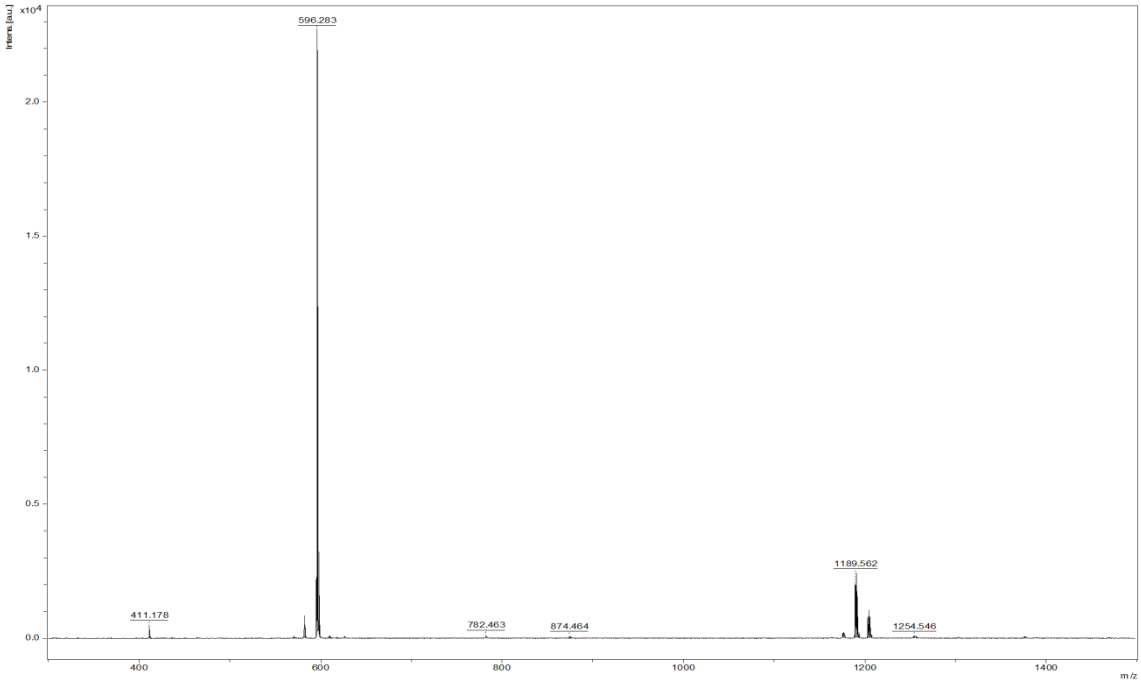

Figure S4. MALDI-TOF mass spectrum of ADPM **4**.

Nuclear Magnetic Resonance spectroscopy

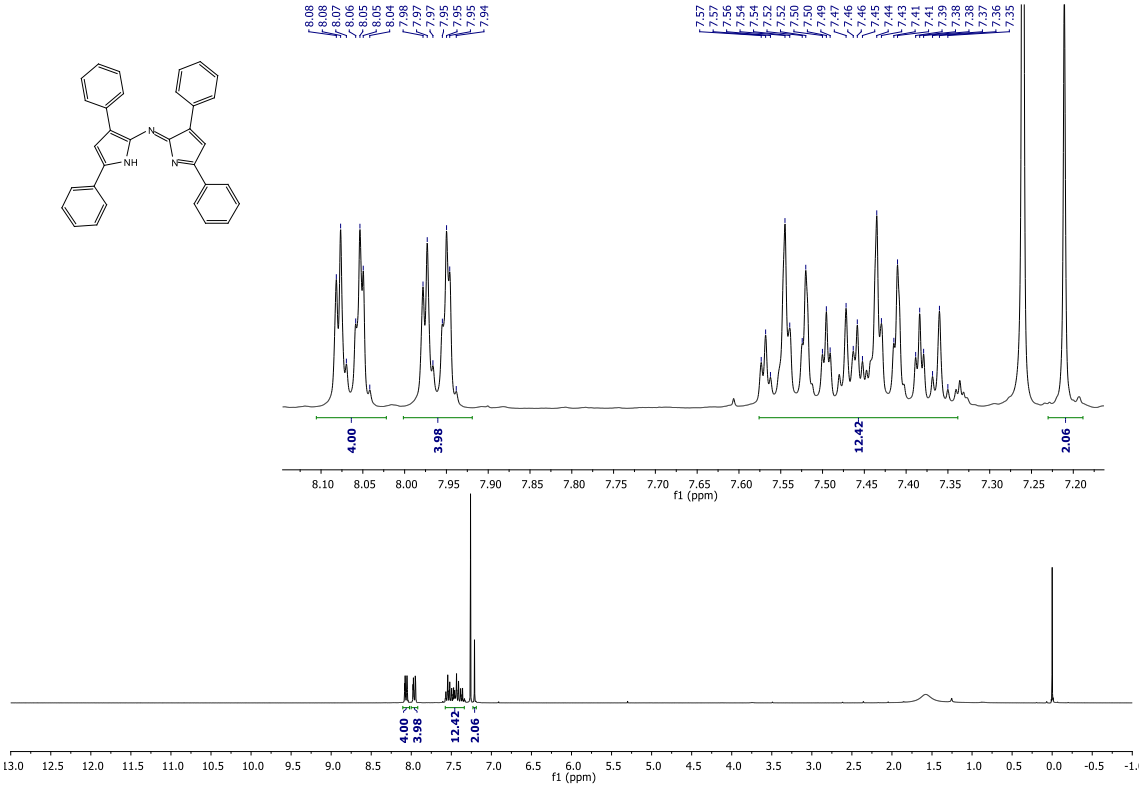

Figure S5. ^{1}H-NMR spectrum of ADPM **1** in $CDCl_3$.

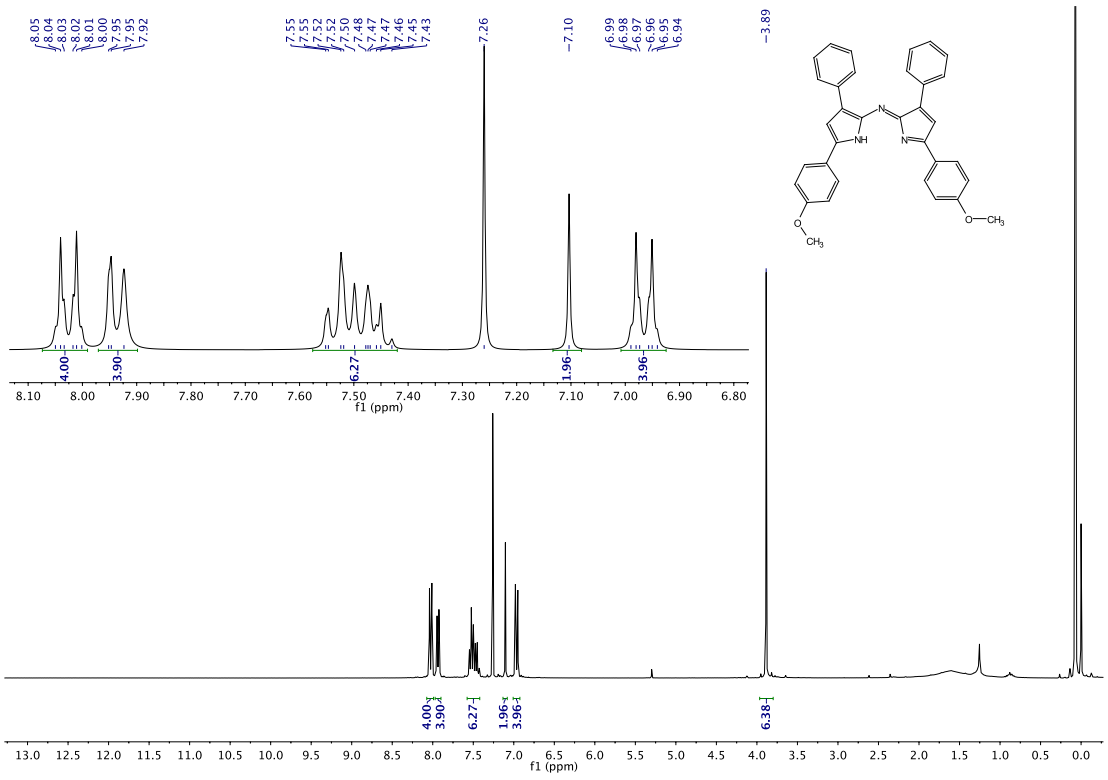

Figure S6.^{1}H-NMR spectrum of ADPM **2** in $CDCl_3$.

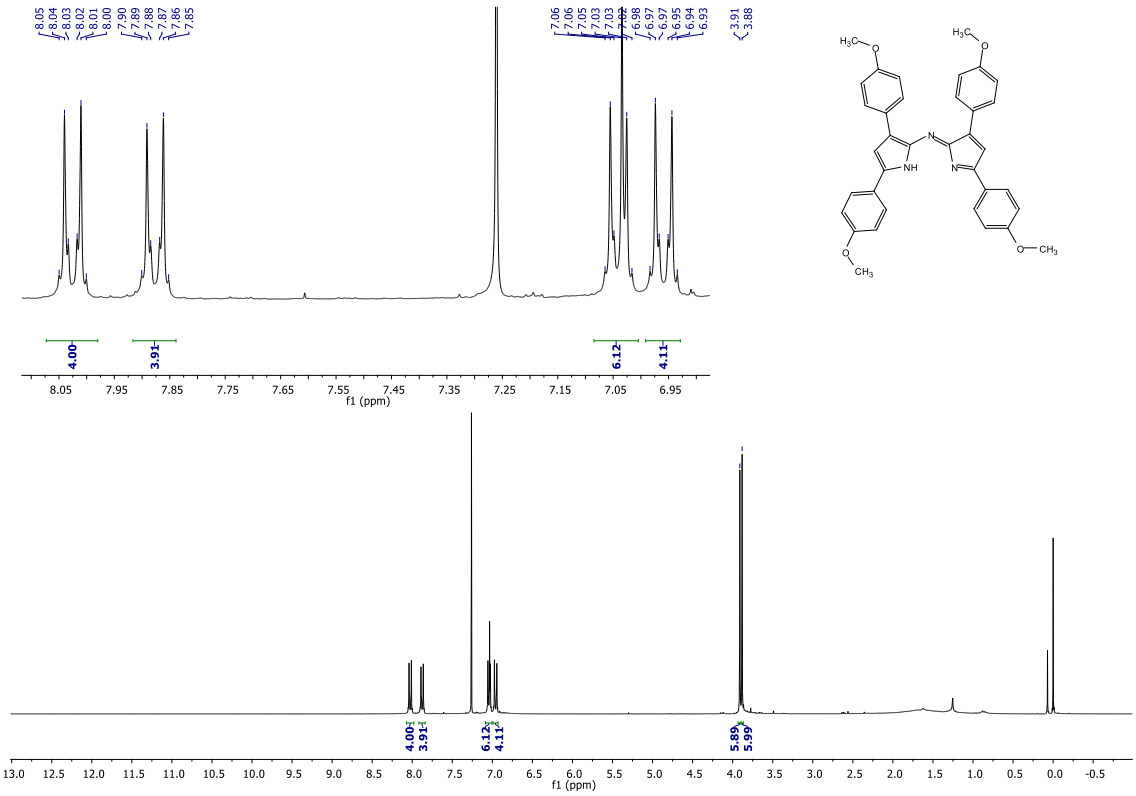

Figure S7. ^{1}H-NMR spectrum of ADPM **3** in $CDCl_3$.

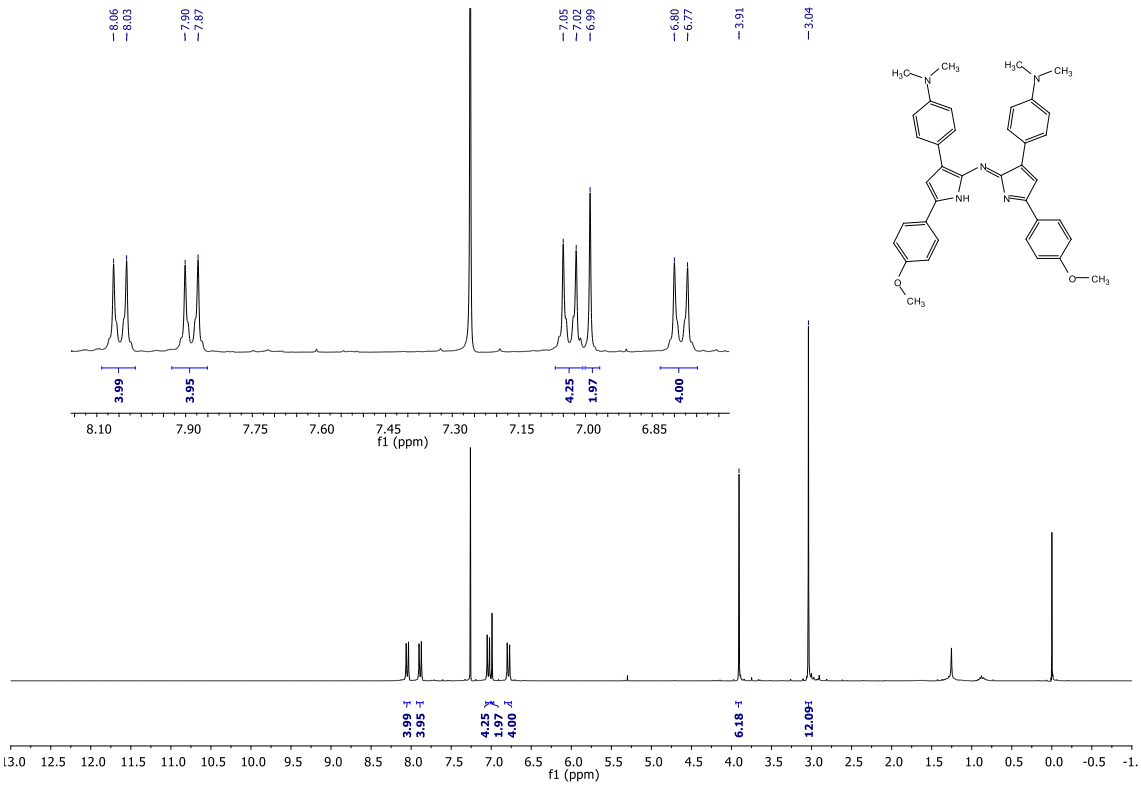

Figure S8.^{1}H-NMR spectrum of ADPM **4** in $CDCl_3$.

Photophysical characterization

UV-Vis and Fluorescence

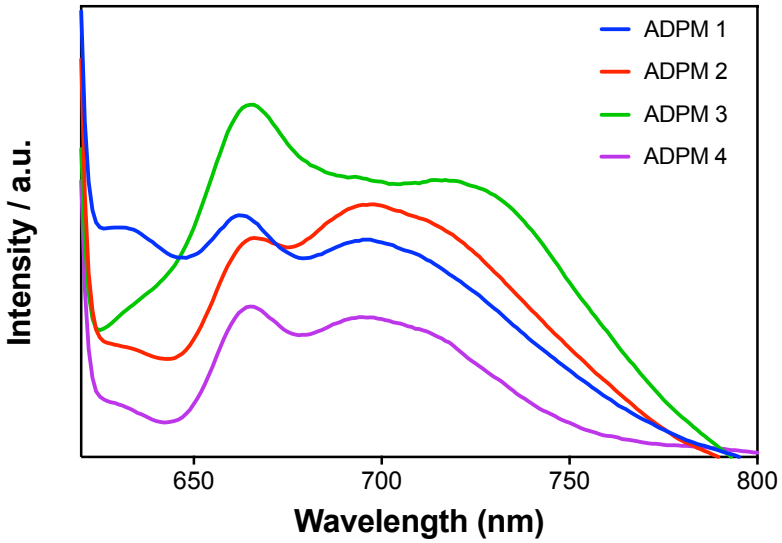

Figure S9. Emission spectra of ADPMs in CH_2Cl_2 solution and excited at 600 nm

Table S1. Photophysical properties of ADPM **1-4** in different solvents.

Solvent	ADPM **1**		ADPM **2**		ADPM **3**		ADPM **4**	
	UV-Vis/nm	Emission[a]/ nm	UV-Vis	Emission[a]	UV-Vis	Emission[a]	UV-Vis	Emission[a]
CH_2Cl_2	306/606	663/701	310/608	668/702	326/657	667/734	327/633	668/701
DMF	306/604	662	302/615	676/695/719	304/632	666/701/775	323/656	732/769
$CHCl_3$	306/603	663/702	307/612	668/704	329/648	667/730	326/632	668/701
DMSO	308/604	663/705	310/618	677/695/723	327/653	667/698/736	327/633	692/730
Ethanol	309/603	647	306/615	713	316/630	775	325/662	777

[a]For the emission spectra, the optical density of all the samples was 0.05 at excitation wavelength. The excitation wavelength was set at the wavelength of maximum absorption.

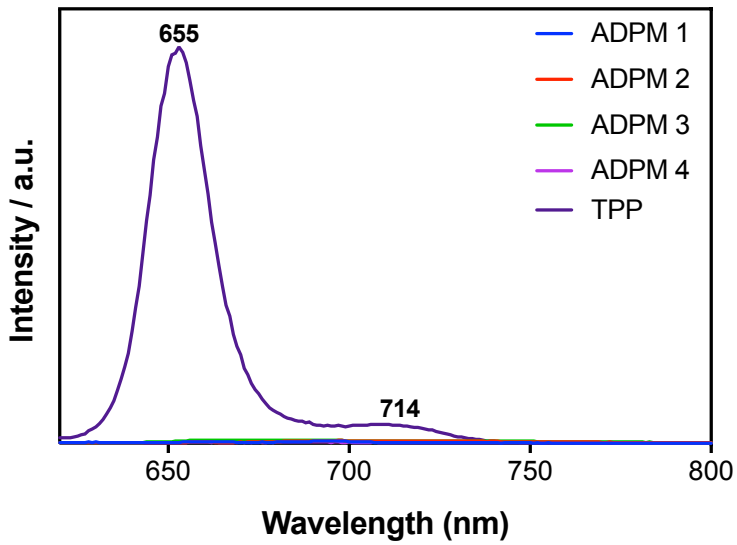

Figure S10. Comparison of the emission spectra of ADPMs **1–4** with the TPP used as fluorescence reference. All spectra were acquired in DMF solutions after excitation at 600 nm.

Drug-likeness properties: Lipinski's Rule of Five

The hydrophobic character of ADPM **1-4** was quantified through the determination of the octanol-water partition coefficient, log *P*. The miLog*P*, as well as other parameters for drug-likeness were evaluated according to the Lipinski's 'rule-of-five', using the Molinspiration WebME Editor 3.81.[2]

All ADPM exhibit values of miLog*P* greater than 5, which constitutes a violation to the Lipinski's rule. This parameter attests the hydrophobic nature of these derivatives and that can result in a poor cell uptake. Although constituting a violation of the Lipinski's rule, this parameter is not enough to exclude the pharmacological potential of a given compound.

Table S2. Comparison of the drug-likeness property/Lipinski's 'rule of five' parameters calculated for ADPM **1-4** and for Foscan®, a photosensitizer with clinical results clearly demonstrated.

Compound	Molecular weight	miLog*P*	*n*-ROTB	*n*-O/N	*n*-OH/NH	*n*-violations	Volume	TPSA
1	449.56	8.41	5	3	1	1	417.76	41.05
2	509.61	8.48	7	5	1	2	468.85	59.52
3	569.66	8.55	9	7	1	2	519.94	77.98
4	595.75	8.60	9	7	1	2	560.66	65.99
Foscan®	680.76	9.07	4	8	6	3	600.39	138.28

n-ROTB, number of rotatable bonds; n-O/N, number of hydrogen acceptors; n-OH/NH, number of hydrogen bond donors; TPSA, topological polar surface area; n-violations, number of violations according to the Lipinski 'rule of five'.

Aggregation studies

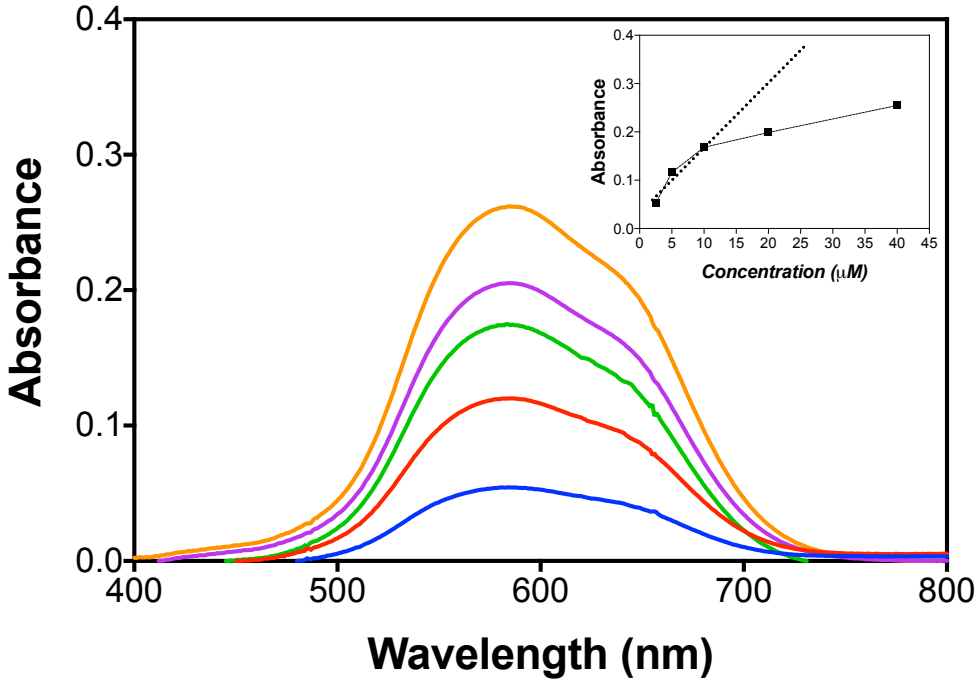

Figure S11. UV-Vis spectra of ADPM **2** at different concentrations in RPMI without phenol red with 1% DMSO. Inset: Plots of the absorbance maxima at 600 nm versus the concentration of ADPM **2** in RPMI with 1% DMSO.

Cytotoxicity assays

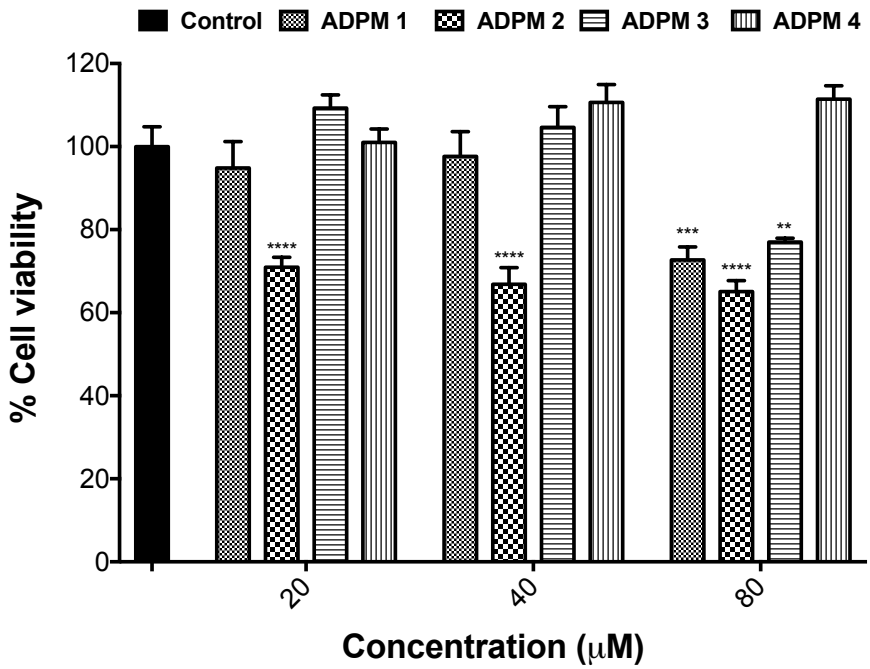

Figure S12. The cytotoxic effect of ADPM **1–4** against B16F10 cells under dark conditions was determined by the MTT assay. All *in vitro* experiments were performed in triplicate and expressed as the mean ± standard deviation. Statistical significance against control cells: **: p value < 0.01; ***p < 0.001 and ****p < 0.0001.

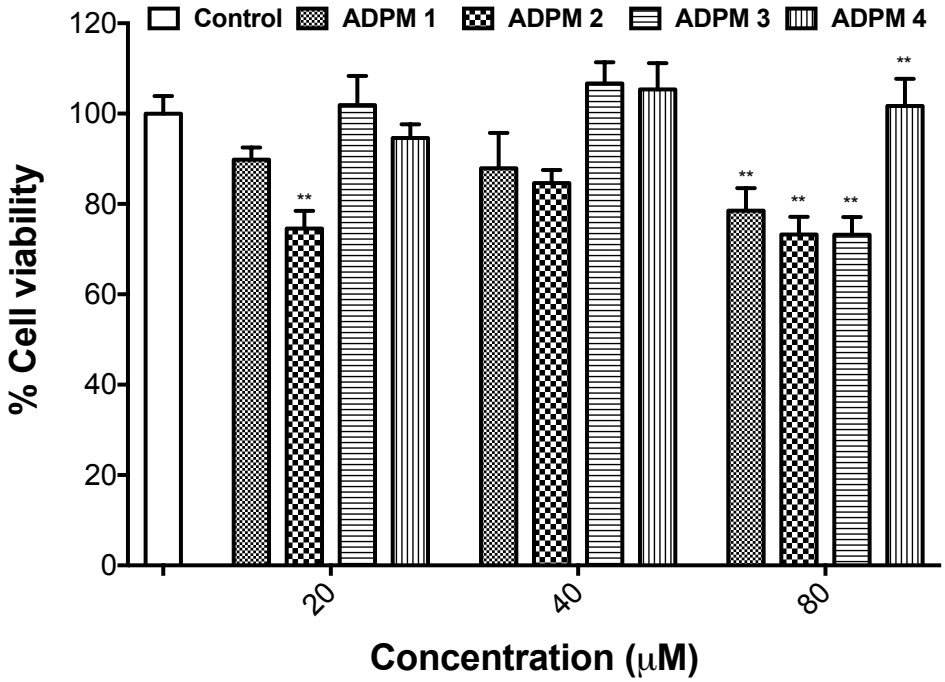

Figure S13. The photodynamic activity of ADPM **1–4** against B16F10 cells was determined by the MTT assay. Cultures were irradiated with a LEDs array with the wavelength set at 640 nm at an irradiance of 13.9 mW/cm^2, and the total light dose of 5 J/cm^2. All *in vitro* experiments were performed in triplicate and expressed as the mean ± standard deviation. Statistical significance: *: p value < 0.05; **p < 0.01 and ****p < 0.0001.

Cellular uptake

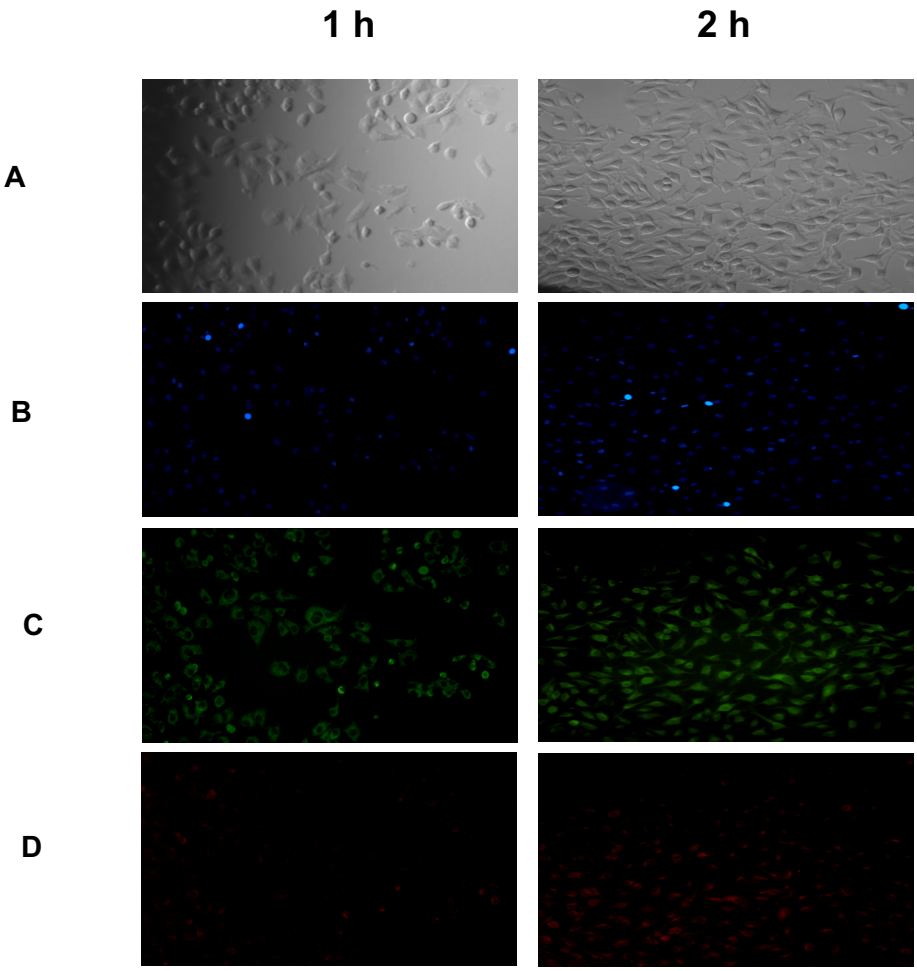

Figure S14. Fluorescence microscopy images of B16F10 cells incubated with ADPM **3** (20 μM) after 1 and 2 h of incubation. (A) Bright field images, (B) Cells marked with Hoechst. Nuclei were labeled with Hoechst dye, (C) Cells marked with Rhodamine 123. Inner mitochondrial membrane was labeled with Rhodamine 123 dye and (D) Red fluorescence of ADPM **3**.

References

1. A. Gorman, J. Killoran, C. O'Shea, T. Kenna, W. M. Gallagher and D. F. O'Shea, *J. Am. Chem. Soc.*, 2004, **126**, 10619-10631.
2. http://www.molinspiration.com (accessed June, 2019).